

The quest for AMS of ^{182}Hf – why poor gas gives pure beams

Martin Martschini^{1,*}, Johannes Lachner¹, Silke Merzel^{1,2,3}, Alfred Priller¹, Peter Steier¹, Anton Wallner^{2,3}, Alexander Wieser¹, and Robin Golser¹

¹University of Vienna - Faculty of Physics, Isotope Physics, VERA Laboratory, Währinger Straße 17, 1090 Vienna, Austria

²Helmholtz-Zentrum Dresden-Rossendorf (HZDR), 01328 Dresden, Germany

³Department of Nuclear Physics, Research School of Physics, Australian National University, Canberra, ACT 2601, Australia

Abstract. The long-lived radioisotope ^{182}Hf ($T_{1/2} = 8.9 \text{ Ma}$) is of high astrophysical interest as its potential abundance in environmental archives would provide insight into recent r-process nucleosynthesis in the vicinity of our solar system. Despite substantial efforts, it could not be measured at natural abundances with conventional AMS so far due to strong isobaric interference from stable ^{182}W . Equally important is an increase in ion source efficiency for the anions of interest.

The new Ion Laser InterAction Mass Spectrometry (ILIAMS) technique at VERA tackles the problem of elemental selectivity in AMS with a novel approach. It achieves near-complete suppression of isobar contaminants via selective laser photodetachment of decelerated anion beams in a gas-filled radio-frequency quadrupole (RFQ) ion cooler. The technique exploits differences in electron affinities (EA) within elemental or molecular isobaric systems neutralizing anions with EAs smaller than the photon energy. Alternatively, these differences in EA can also facilitate anion separation via chemical reactions with the buffer gas.

We present first results with this approach on AMS-detection of ^{182}Hf . With $\text{He} + \text{O}_2$ mixtures as buffer gas in the RFQ, suppression of $^{182}\text{WF}_5^-$ vs $^{180}\text{HfF}_5^-$ by $>10^5$ has been demonstrated. Mass analysis of the ejected anion beam identified the formation of oxyfluorides as an important reaction channel. The overall Hf-detection efficiency at VERA presently is 1.4 % and the W-corrected blank value is $^{182}\text{Hf}/^{180}\text{Hf} = (3.4 \pm 2.1) \times 10^{-14}$. In addition, a survey of different sample materials for highest negative ion yields of HfF_5^- with Cs-sputtering has been conducted.

1 Introduction

Accelerator mass spectrometry (AMS) commonly is the most sensitive technique for the detection of long-lived isotopes, reaching down to the attogram/gram abundance range. Over recent years, it has subsequently been employed in the search for signatures from recent nucleosynthesis in the vicinity of the solar system and corresponding signals of ^{60}Fe and ^{244}Pu have been identified in terrestrial and lunar archives [1–5]. The observed scarcity of ^{244}Pu has fueled the discussion about the astrophysical site of the rapid neutron-capture process (r-process) in favor of neutron star mergers [6]. Currently, this is the only experimentally confirmed r-process production site following gravitational wave detection GW170817 [6] and spectroscopic observation of the associated kilonova SSS17a (e.g. [7]). However, unexplained discrepancies with astronomical observations remain and suggest further sites and possibly multiple r-process components (see [8] for a recent review).

An important anchor point in this puzzle is ^{182}Hf with a half life of $T_{1/2} = (8.90 \pm 0.09) \text{ Ma}$ [9]. As is the case for ^{60}Fe and ^{244}Pu , there is no natural production of ^{182}Hf on Earth and all of the primordial contribution has long since decayed away. Thus, any ^{182}Hf detected must stem from

recent nucleosynthesis. Since ^{182}Hf is in the middle-mass region of the r-process nuclides, it could potentially be produced in different scenarios to those for ^{244}Pu . Based on various yield- and elemental-ratio-calculations for possible ^{182}Hf production scenarios [10–13], the estimated $^{182}\text{Hf}/\text{Hf}$ signal intensity is at most a few times 10^{-13} , but could even be one to three orders of magnitude lower depending on the Hf incorporation efficiencies and stable Hf content in the archives.

The challenge in AMS-detection of ^{182}Hf at these low abundances is interference from the ubiquitous stable isobar ^{182}W . This quest started at the 3-MV-Vienna Environmental Research Accelerator (VERA) in 2002 [14]. It soon turned out that extraction of HfF_5^- from a HfF_4 sample matrix provided a W-suppression $>10^3$, but no further separation could be achieved with subsequent AMS-filters or single ion detectors [15]. The resulting detection limit was roughly $^{182}\text{Hf}/\text{Hf} = 1 \times 10^{-11}$, but very susceptible to the W-content of the sputter matrix and the ion source materials [15, 16]. The high mass of the isobars and their relatively low $\Delta Z/Z$ complicate isobar separation by conventional means like differences in energy loss characteristics or gas-filled-magnets [17]. Despite some progress with innovative detector concepts [18], no better detection limits have yet been achieved at larger tandem facilities [19]. A novel approach at VERA making use of differ-

* e-mail: martin.martschini@univie.ac.at

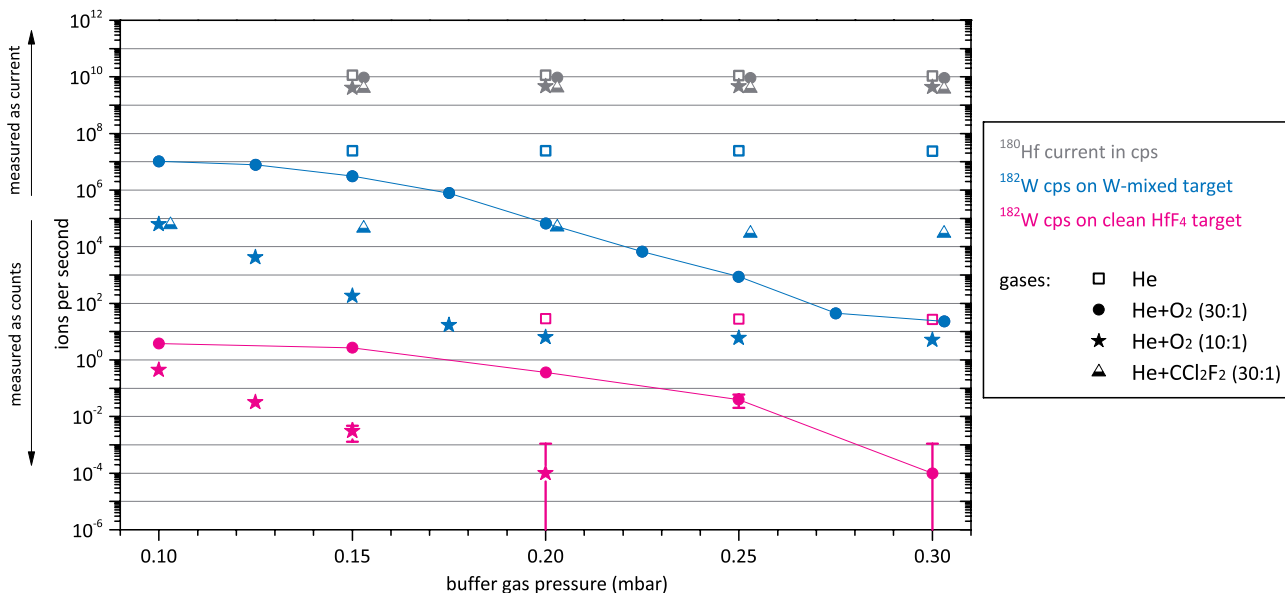


Figure 1. Ion intensities of $^{180}\text{HfF}_5^-$ and $^{182}\text{WF}_5^-$ transmitted through the ILIAMS cooler as a function of buffer gas pressure for various gases. The respective ion species were measured as $^{180}\text{Hf}^{3+}$ and $^{182}\text{W}^{3+}$ in a Faraday cup or an ionization chamber detector on the high-energy side of VERA. Plotted intensities are corrected for the effective charge state yield of 20 % (including accelerator transmission). Lines between symbols are to guide the eye.

ences in electron affinities (EAs) between the isobars may, however, allow us to reach the required sensitivity.

2 Isobar suppression in the ILIAMS setup

2.1 Setup and Electron Affinities

The Ion Laser InterAction Mass Spectrometry (ILIAMS) setup is the central part of a new injector at the VERA facility dedicated to element selective filtering by laser photodetachment; a recent description of the layout is given in [20]. It consists of a cesium sputter ion source followed by a 90° bending magnet and the ILIAMS radiofrequency quadrupole ion cooler, a 1 m long linear ion guide based on a 2D Paul trap, where electrostatically-slowed anions gently collide with He buffer gas and reach almost thermal energies resulting in transit times of several ms [21]. Inside the ion cooler, the ion beam is co-linearly overlapped with an intense cw- or quasi-cw laser beam. All anions with EAs smaller than the photon energy are thereby efficiently neutralized while anions with EAs larger than the photon energy remain unaffected. This novel technique works extraordinarily well and provides isobar suppression factors of 10^{11} and 10^{12} for $^{36}\text{S}^-$ vs $^{36}\text{Cl}^-$ and $^{26}\text{MgO}^-$ vs $^{26}\text{AlO}^-$, respectively [20, 22].

For Hf, optical filtering has not been implemented so far since no experimental data for the EAs of HfF_5^- and WF_5^- exist. Theoretical calculations suggest that EAs are suitable and lie in the UV, with calculated vertical detachment energies of 3.9 eV for WF_5^- and 8.8 eV for HfF_5^- [23]. The only experimental anchor point so far is the finding that the detachment cross section of WF_5^- is a factor of 100 higher than that of HfF_5^- with a 266 nm laser (photon energy 4.66 eV) [24].

2.2 Gas reaction studies

Differences in electronic structure of anions can also be exploited in anion-gas reactions at eV energies and O_2 was found particularly well suited for HfF_5^- - WF_5^- separation, providing an isobar suppression of at least 10^3 in an earlier study [25]. While the exact reaction channel remained elusive, Zhao et al. [25] argued that HfF_5^- , being a superhalogen anion, is extraordinarily stable and, thus, highly immune to electron charge transfer reactions, collisional detachment and association or transformation of molecules at eV energies.

Similar experiments have now been conducted at ILIAMS using gas mixtures of $\text{He}+\text{O}_2$ and $\text{He}+\text{CCl}_2\text{F}_2$. The respective buffer gases were volumetrically pre-mixed in a 12 liter gas bottle. For each buffer gas, the system was first tuned for optimum $^{180}\text{HfF}_5^-$ transmission at 0.20 mbar pressure at the buffer gas inlet and then the pressure was varied while measuring the respective ion species as $^{180}\text{Hf}^{3+}$ and $^{182}\text{W}^{3+}$ in a Faraday cup or an ionization chamber detector on the high-energy side of VERA (Fig. 1). Sputter targets contained mixed powders of $\text{HfF}_4+\text{PbF}_2+\text{Ag}$ (1:1:1 by weight) and $\text{HfF}_4+\text{W}+\text{PbF}_2+\text{Ag}$ (1:1:1:1 by weight), and the ion source produced typically 50–300 nA of $^{180}\text{Hf}^-$ (from either material) and 100–500 pA of $^{182}\text{WF}_5^-$, respectively.

While $^{180}\text{HfF}_5^-$ transmissions are almost identical for pure He and $\text{He}+\text{O}_2$ (30:1), the amount of $^{182}\text{WF}_5^-$ transmitted through $\text{He}+\text{O}_2$ (30:1) is a factor of 10^6 lower compared to pure He. Accounting for the total ILIAMS transmission of 35% for $^{180}\text{HfF}_5^-$ (cf. 3.2), this translates into an isobar suppression of 3×10^5 . Raising the O_2 content of the buffer gas to $\text{He}+\text{O}_2$ (10:1) provides stronger destruction of $^{182}\text{WF}_5^-$ at lower buffer gas pressures but at higher pressures the intensity of $^{182}\text{WF}_5^-$ reaches a plateau at al-

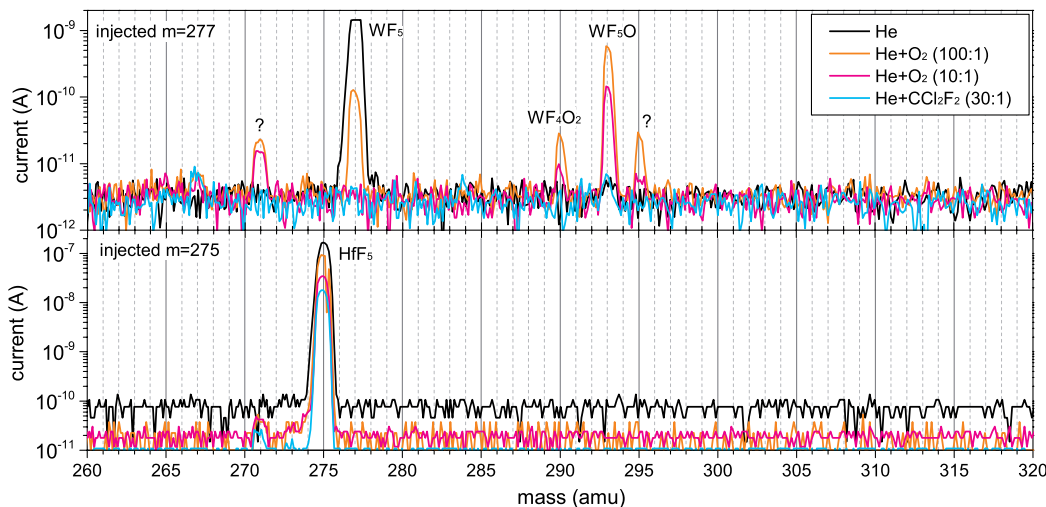


Figure 2. Mass scans of the anion beam extracted from the ILIAMS ion cooler operated with different buffer gases at an inlet buffer gas pressure of 0.30 mbar for all scans. The top graph shows the mass spectrum when injecting $^{182}\text{WF}_5^-$ ($m=277$), the bottom one when injecting $^{180}\text{HfF}_5^-$ ($m=275$). For better mass resolution, the current was measured in the Faraday cup directly following the VERA tandem accelerator. Plotted currents are thus convoluted with the charge-state distribution and do not represent primary anion beam intensities. Variations in background stem from different sensitivities of the current amplifier (model SRS-SR570).

most the same level as with $\text{He}+\text{O}_2$ (30:1). This yet unexplained plateau effect has been observed in e.g. [26] as well and we attribute it to reverse reactions in the gas. With laser photodetachment, no such effects have been observed so far. The transmission of $^{180}\text{HfF}_5^-$ with $\text{He}+\text{O}_2$ (10:1) is significantly reduced to around half of that with pure He. Since these losses are independent of the buffer gas pressure and, thus, the ion transit time through the gas, they are most likely associated with collisional detachment on O_2 leaking into the electrostatic de- and acceleration areas between the cooler apertures and the first aperture lenses, where ions have hundreds of eV energy. The same is true for $\text{He}+\text{CCl}_2\text{F}_2$ (30:1) with even slightly higher loss of $^{180}\text{HfF}_5^-$. The amount of transmitted $^{182}\text{WF}_5^-$ is reduced by 10^3 , but also independent of buffer gas pressure, and hence not in anion-gas reactions at eV energies.

In order to pin down reaction channels and identify negatively-charged reaction products, the anion beam extracted from the ion cooler was mass-analyzed in the range of 250 – 320 amu using VERA’s injection magnet (Fig. 2).

With pure He, only the respective ion species $^{180}\text{HfF}_5^-$ and $^{182}\text{WF}_5^-$ are detected. Indeed, for an injection mass of 275 ($^{180}\text{HfF}_5^-$), the same is true for the other gases as well with no associated or transformed molecules being observed at any other mass. Significant oxyfluoride formation occurs when injecting $^{182}\text{WF}_5^-$ through an O_2+He mixture, with an intense peak at mass 293 corresponding to $^{182}\text{WF}_5\text{O}^-$ being visible. With $\text{He}+\text{O}_2$ (100:1), the intensity of this peak explains at least half of the deficit in $^{182}\text{WF}_5^-$ compared to pure He. This is in agreement with earlier studies [20]. A second peak at mass 290 is attributed to the formation of $^{182}\text{WF}_4\text{O}_2^-$, albeit with lower intensity. Further peaks are observed at masses 271 and 295, however, their origin remains unsettled so far. The latter might indicate the formation of $^{182}\text{WF}_3\text{O}_2^-$, but a very weak signal contradicting this explanation also seems

to be present in the Hf-scans with $\text{He}+\text{O}_2$. Higher oxygen contents in the buffer gas ($\text{He}+\text{O}_2$ 10:1) produce the same peaks, although their intensity is significantly lower, thus other mechanisms like resonant charge transfer or collisional detachment, either directly with the analyte species or with formed molecules, are likely to reduce the anion intensity.

$\text{He}+\text{CCl}_2\text{F}_2$ (30:1) does not yield any transmitted W-anions above the sensitivity limit of the Faraday cup (10 pA), thus, no significant association of molecules is observed, which is in agreement with above conclusions of pure collisional detachment. A mixture $\text{He}+\text{O}_2+\text{CCl}_2\text{F}_2$ (150:1:1) produced the same oxyfluoride peaks as $\text{He}+\text{O}_2$, but at much lower intensity. In all cases no formation of WF_6^- or WF_7^- was observed. Whether the fluorine atoms are too strongly bound in CCl_2F_2 to be available for reactions and other gases with weaker-bound fluorine potentially allow this reaction path remains to be investigated.

3 AMS measurements and results

3.1 Sample preparation chemistry

Samples under investigation in this study were from commercial high-purity HfF_4 material (Alfa Aesar, purity >99.9%) or reference materials from earlier campaigns [15, 16]. In parallel, a sample preparation procedure has been developed to allow ^{182}Hf analysis from neutron-irradiated W. Basic steps are:

- 1.) Dissolving W in 2 ml HNO_3 (70%)/ 2.5 ml HF (48%; drop-by-drop; cooling);
- 2.) Addition of 1 mg natural Hf as solution;
- 3.) BaHfF_6 -precipitation by 0.5 ml saturated $\text{Ba}(\text{NO}_3)_2$ solution [27];
- 4.) Dissolving in HNO_3 (~35%) saturated with H_3BO_3 [27];

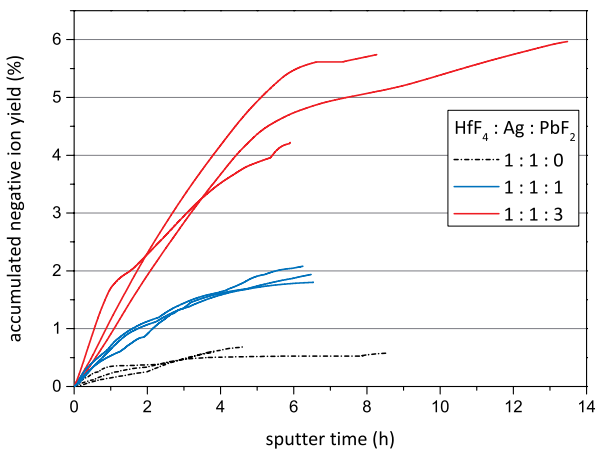


Figure 3. Cumulative negative ion yield of HfF_5^- as a function of sputter time for targets filled with powders of HfF_4 , Ag and PbF_2 mixed in three different weight ratios. Ions were collected as $^{180}\text{HfF}_5^-$ in a Faraday cup. Three sputter targets of each sample material were measured.

- 5.) $\text{Hf}(\text{OH})_4$ precipitation by $\text{NH}_{3\text{aq}}$;
- 6.) Dissolving in 2 ml 0.5 M $\text{HCl}/0.5$ M HF;
- 7.) Ion exchange (2 ml DOWEX 1x8, 100-200 mesh [28] [29]): Hf in 7 ml 9 M $\text{HCl}/0.01$ M HF;
- 8.) $\text{Hf}(\text{OH})_4$ precipitation by $\text{NH}_{3\text{aq}}$;
- 9.) Dissolving in 100 μl HF (24%);
- 10.) Drying at room temperature and 80°C.

The ion exchange described in [28] [29] has been further optimized for higher Hf-yield using inductively coupled plasma mass spectrometry (ICP-MS). A sufficient decontamination factor of $>10^8$ could be reached with chemical yields of 91–100%, thus making the production of a 1–2 mg HfF_4 -target with a W-content of $<10 \mu\text{g/g}$ starting from a 1 g W matrix feasible. The use of Suprapur® chemicals has proven necessary as otherwise remaining W traces clearly originate from chemical products and consumables. Variants of this procedure will be applied for environmental samples in future studies. All HfF_4 materials for chemistry tests have been mixed (1:3 by weight) with PbF_2 (Alfa Aesar Puratronic®, >99.997% purity) and pressed in Cu cathodes; future samples will be additionally mixed with Ag for more stable sputter rates. Single BaHfF_6 precipitation yields $\sim 10^4$ as decontamination factor, which is not sufficient in most cases. Furthermore, BaHfF_6 , a sputter material suggested by [19], was found to quickly poison the ionizer and the current output from the source dropped by at least a factor of 100 within a few minutes of sputtering.

3.2 AMS detection efficiency

As for any low-level AMS measurement, the overall detection efficiency of ^{182}Hf is a crucial parameter and highest losses generally occur in the production of negative ions in the Cs sputter ion source. Therefore, a study of the HfF_5^- ionization yield with different admixing ratios of PbF_2 powder to the final sputter matrix was conducted.

Batches of sputter targets containing known amounts of typically 1–4 mg HfF_4 were prepared and sputtered to exhaustion while collecting the $^{180}\text{HfF}_5^-$ current in the Faraday cup right after the first bending magnet (Fig. 3). Of the three mixtures tested, the best HfF_5^- yields are achieved with highest PbF_2 admixture, i.e. $\text{HfF}_4+\text{Ag}+\text{PbF}_2$ 1:1:3 by weight. Within the first two hours of sputtering, 2% of the sample material was turned into HfF_5^- , peaking at finally about 6%. On the other hand, increasing the proportion of PbF_2 results in higher WF_5^- formation from the target material, as demonstrated in [16]. The study here was conducted with ultrapure commercial HfF_4 and in first tests, no enhanced WF_5^- content in the anion beam was observed (cf. 3.3). For real environmental samples with a slightly elevated W-content, it might however be necessary to determine the optimum PbF_2 mixing ratio as a trade-off between high HfF_5^- and still strong WF_5^- suppression in the ion source. For these reasons, an ionization yield of only 2% achievable with low admixture (1:1) of PbF_2 is assumed for the considerations below.

The transmission of $^{180}\text{HfF}_5^-$ through the ion cooler is 35% at an injected current of 200 nA. In contrast to e.g. Cl, where the cooler transmission is limited by the total charge limit of the RFQ ion guide [20], losses of HfF_5^- are mostly caused by the large emittance of the ion beam from the ion source. The intense F^- current from the sample on the order of 50 μA blows up the size of the entire ion beam between the source and first mass-separation in the magnet. Therefore, even the mass-separated ion beam becomes too large to fit through the 3 mm entrance aperture of the ion cooler. Subsequently, this issue cannot be overcome by attenuation of the stable reference isotope beam but would require a redesign of the cooler injection optics, which is yet beyond our scope. In addition, around $\sim 15\%$ of the HfF_5^- beam is lost in collisional detachment with O_2 leaking into the injection and extraction area of the cooler.

The tandem accelerator is operated at 2.4 MV with He as stripper gas providing an effective 3+ charge state yield of 20 %. The resulting 8.8 MeV $^{182}\text{Hf}^{3+}$ ion beam is directed without losses into a split anode ionization chamber with a $10 \times 10 \text{ mm}^2$ large, 100 nm thick silicon nitride entrance window. Since no W isobar separation is achieved within the ionization chamber, virtually all events fall within the wide ROI of the 3+ charge state, thus, the detector efficiency is close to 100%. Stable $^{180}\text{Hf}^{3+}$ is measured in the Faraday cup following the analyzing magnet.

The performance is summarized in Table I and results in an overall Hf detection efficiency of $>1.4\%$. Assuming that at least 30 events need to be collected in

Table 1. Summary of Hf detection efficiency

negative ion yield	> 2%
ILIMAMS cooler transm. $\text{He}+\text{O}_2$ at 200 nA	35%
low-energy transport efficiency	100%
accelerator transm. and 3+ charge state yield	20%
high-energy transport efficiency	100%
ionization chamber efficiency	100%
overall detection efficiency	>1.4‰

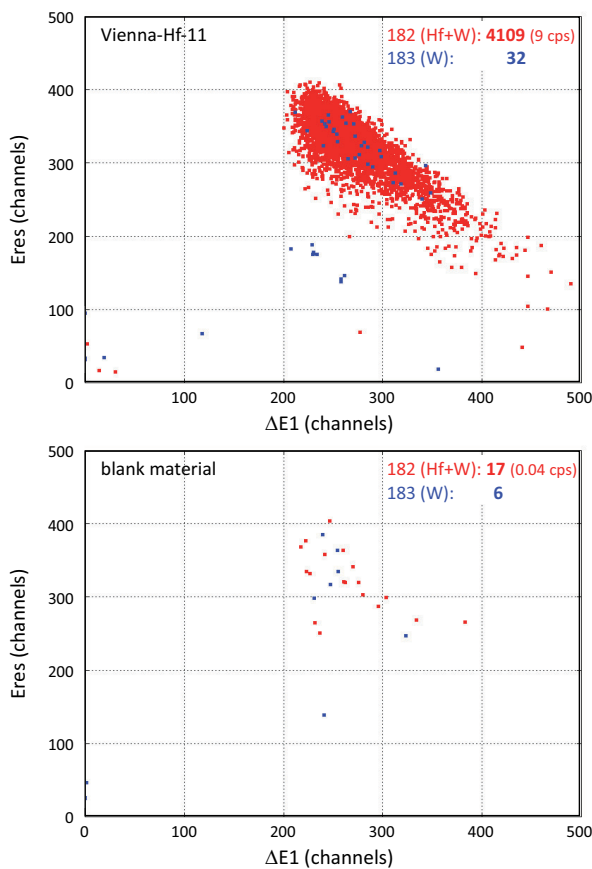


Figure 4. Detector spectra of runs on Vienna-Hf-11 reference material with a nominal ratio of $^{182}\text{Hf}/^{180}\text{Hf} = 5.88 \times 10^{-11}$ and a blank material containing no ^{182}Hf . Red events were collected with the system tuned for mass 182 (i.e. $^{182}\text{Hf}^{3+}$ and $^{182}\text{W}^{3+}$), blue events for mass 183 (only $^{183}\text{W}^{3+}$ and m/q ambiguities). The acquisition time was 455 s in all cases. There is a strong surplus of m=182-events on the reference material.

the detector for an unambiguous ^{182}Hf signal identification, we presently require 2.2×10^4 ^{182}Hf atoms in the sputter sample. In a 1 mg Hf sample, this corresponds to an implied theoretical abundance sensitivity level of $^{182}\text{Hf/Hf} = 1.8 \times 10^{-14}$ if isobaric interferences can effectively be fully suppressed.

3.3 Results of first AMS measurements

First AMS measurements were conducted on a set of inhouse reference materials also employed in [16] with nominal ratios of $^{182}\text{Hf}/^{180}\text{Hf} = 5.59 \times 10^{-10}$ (now labeled Vienna-Hf-10) and $^{182}\text{Hf}/^{180}\text{Hf} = 5.88 \times 10^{-11}$ (Vienna-Hf-11) and blank material from commercial HfF_4 (Alfa Aesar). Very recent measurements suggest that both reference materials might in fact have (2.0 ± 0.2) -times higher ratios and certainly require thorough remeasurement and cross-calibration in the very near future. For the following evaluation, the above nominal values were used. Hence, all measured Hf-ratios may require scaling by this factor once the proper isotopic ratios of these materials have been determined.

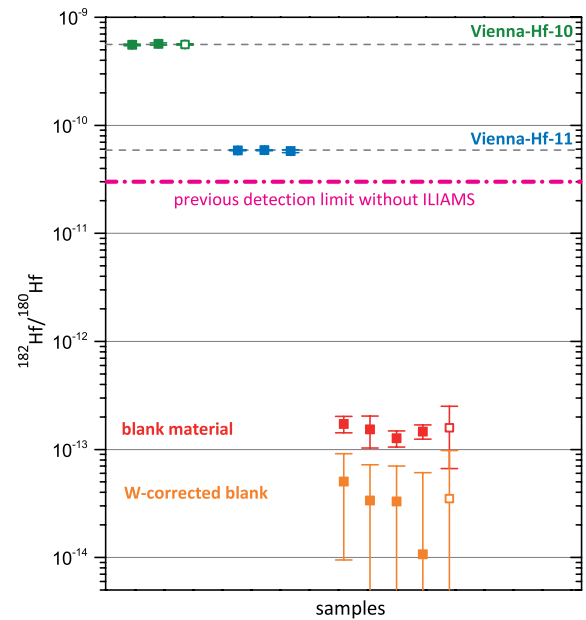


Figure 5. AMS measurement results for samples with Vienna-Hf-10 and Vienna-Hf-11 reference materials with nominal ratios of $^{182}\text{Hf}/^{180}\text{Hf} = 5.59 \times 10^{-10}$ and $^{182}\text{Hf}/^{180}\text{Hf} = 5.88 \times 10^{-11}$, respectively, as well as blank material from commercial HfF_4 containing no ^{182}Hf . All results have been normalized to the Vienna-Hf-10 reference material. Filled symbols indicate that PbF_2 was admixed to the sample matrix by weight 1:1 to HfF_4 , open symbols indicate no addition of PbF_2 . Each datapoint is the average of one sputter target over multiple runs.

During the measurements, the ILIAMS cooler was operated at 0.30 mbar He+O₂ (30:1) buffer gas pressure. Sample spectra from the split anode ionization chamber are shown in Fig. 4. Measured $^{180}\text{Hf}^{3+}$ -currents were typically 30–40 nA. Since $^{182}\text{Hf}^{3+}$ and $^{182}\text{W}^{3+}$ cannot be distinguished in the ionization chamber, the amount of $^{182}\text{W}^{3+}$ is monitored via separately counting $^{183}\text{W}^{3+}$ and subsequent correction for the ^{182}W -contribution to the m=182 signal [15]. The $^{182}\text{W}/^{183}\text{W}$ seen by the detector is experimentally determined on samples contaminated with W on purpose at the 1000 µg/g level and was 2.43 ± 0.21 for the first measurement in comparison to the natural ratio of 1.85. Different masses are injected sequentially by adjusting the field of the ILIAMS bending magnet, the voltage of the insulated chamber of the injection magnet before the accelerator and the accelerator terminal voltage with switching times of ~3 s. Each run consists of four sequences for determination of the stable reference isotope currents in 5 s and in between 3 pairs of counting sequences for masses 182 (~150 s) and 183 (variable, here ~150 s). The system ran automatically and unattended for three days.

Final results normalized to the Vienna-Hf-10 reference material are plotted in Fig. 5. The reproducibility for the Vienna-Hf-11 material is better than 5% and in agreement with its nominal value. After correction of the W-induced background, the average blank value is $^{182}\text{Hf}/^{180}\text{Hf} = (3.4 \pm 2.1) \times 10^{-14}$. The upper limit translates into a present detection limit of $^{182}\text{Hf/Hf} \approx 6 \times 10^{-14}$, which

is at least a 170-fold improvement compared to previous work [16, 19]. Interestingly, no statistically significant difference in W-induced background has been observed between targets with admixture of PbF_2 and the one without. This is rather surprising considering the strong dependence of the $\text{WF}_5^-/\text{HfF}_5^-$ ratio on F-availability in the sputter matrix observed in Ref. [16]. In our view, it indicates that for commercial HfF_4 a significant part of the W in the ion beam extracted from these samples does not originate from the sputter matrix itself (in agreement with findings in Ref. [16]), but further investigations are certainly necessary. Cross contamination and memory effects in the ion source have not been observed above this background so far.

4 Conclusions and Outlook

Significant progress has been achieved in AMS of ^{182}Hf by using reactive gases in an RFQ ion cooler and the mechanisms underlying the W-suppression have been studied. Despite an improvement in sensitivity by more than two orders of magnitude compared to previous work, estimations suggest that the detection of live nucleosynthesis signals remains still challenging and can presently only be expected for the high- $^{182}\text{Hf}/\text{Hf}$ -signal scenarios. The EAs of molecular anions are promising to implement optical filtering by means of a suitable laser in the near future. This should provide the missing one to two orders of magnitude in isobar suppression required to reach the sensitivity deemed necessary for low-signal scenarios. Within the next months, the ILIAMS setup will be used to determine the $^{186}\text{W}(\text{n},\text{n}\alpha)^{182}\text{Hf}$ cross section on samples irradiated with MeV neutrons, where $^{182}\text{Hf}/\text{Hf}$ -ratios of at least 2×10^{-12} are expected.

Acknowledgements

The authors are grateful to Sabrina Beutner (HZDR), Sophie Neumayer (U Vienna) and Anastassiya Tchaikovsky (U Vienna) for ICP-MS measurements of Hf and W; Steve Tims (ANU), Carsten Münker (U Cologne) and Jan Welch (Tu Vienna) for help in the chemistry lab and/or discussion; Max Bichler (TU Vienna) for chemical preparation of the reference materials and for valuable advice. The VERA team acknowledges financial support of the ILIAMS research activities by "Investitionsprojekte" of the University of Vienna. R.G. acknowledges support by "ChETEC" COST Action (CA16117).

References

- [1] K. Knie, G. Korschinek, T. Faestermann *et al.*, Phys. Rev. Lett. **93**, 171103 (2004).
- [2] L. Fimiani, D. L. Cook, T. Faestermann *et al.*, Phys. Rev. Lett. **116**, 151104 (2016).
- [3] A. Wallner, T. Faestermann, J. Feige *et al.*, Nature Comm. **6**, 5956 (2015).
- [4] A. Wallner, J. Feige, N. Kinoshita *et al.*, Nature **532**, 69–72 (2016).
- [5] D. Koll, G. Korschinek, T. Faestermann *et al.*, Phys. Rev. Lett. **123**, 072701 (2019).
- [6] B. P. Abbott *et al.* (LIGO Scientific Coll. and Virgo Coll.), Phys. Rev. Lett. **119**, 161101 (2017).
- [7] B. P. Abbott, R. Abbott, T. D. Abbott *et al.*, Astrophys. J. Lett. **848**, L12 (2017).
- [8] J. J. Cowan, Ch. Sneden, J. E. Lawler *et al.*, arXiv 1901.01410 (2019).
- [9] C. Vockenhuber, F. Oberli, M. Bichler *et al.*, Phys. Rev. Lett. **93**, 0172501 (2004).
- [10] M. Lugaro, A. Heger, D. Osrn *et al.*, Science **345** 650–653 (2014).
- [11] T. Rauscher, A. Heger, R. D. Hoffman *et al.*, Astrophys. J. **576**, 323–348 (2002).
- [12] S. Goriely, H.-Th. Janka, Mon. Not. Roy. Astron. Soc. **459**, 4174–4182 (2016).
- [13] B. J. Fry, B. D. Fields, J. R. Ellis, Astrophys. J. **800**, 71 (2015).
- [14] C. Vockenhuber, I. Ahmad, R. Golser *et al.*, Int. J. Mass Spec. **223–224**, 713–732 (2003).
- [15] C. Vockenhuber, M. Bichler, R. Golser *et al.*, Nucl. Instrum. Methods B **223–224**, 823–828 (2004).
- [16] O. Forstner, H. Gnaser, R. Golser *et al.*, Nucl. Instrum. Methods B **269**, 3180–3182 (2011).
- [17] H.-A. Synal, Int. J. Mass Spec. **349–350**, 192–202 (2013).
- [18] C. Vockenhuber, A. Bergmaier, T. Faestermann *et al.*, Nucl. Instrum. Methods B **259**, 250–255 (2007).
- [19] C. Vockenhuber, C. Feldstein, M. Paul *et al.*, New Astron. Rev. **48**, 161–164 (2004).
- [20] M. Martschini, D. Hanstorp, J. Lachner *et al.*, Nucl. Instrum. Methods B **456**, 213–217 (2019).
- [21] M. Martschini, J. Pitters, T. Moreau *et al.*, Int. J. Mass Spec. **415**, 9–17 (2017).
- [22] J. Lachner, C. Marek, M. Martschini *et al.*, Nucl. Instrum. Methods B **456**, 163–168 (2019).
- [23] H. Chen, P. Andersson, A. O. Lindahl *et al.*, Chem. Phys. Lett. **511(4–6)**, 196–200 (2011).
- [24] T. Leopold, J. Rohlén, P. Andersson *et al.*, Int. J. Mass Spec. **359**, 12–18 (2014).
- [25] X.-L. Zhao, J. Eliades, A. E. Litherland *et al.*, Rap. Comm. Mass Spec. **27**, 2818–2822 (2013).
- [26] J. A. Eliades, X.-L. Zhao, A. E. Litherland *et al.*, Nucl. Instrum. Methods B **361**, 294–299 (2015).
- [27] E. Merz, Geochim. Cosmochim. Acta **26**, 347–349 (1962).
- [28] M. F. Horan, M. I. Smoliar, R. J. Walker, Geochim. Cosmochim. Acta **62(3)**, 545–554 (1998).
- [29] T. Kleine, C. Münker, K. Mezger *et al.*, Nature **418**, 952–955 (2002).